

# SYNTHESIS AND CHARACTERIZATION OF $Zn_{1-x}Al_xO$ OXIDE NANOMATERIALS

## Abstract

Zinc Oxide (ZnO) nanopowders with different ratios of zinc oxide replaced with aluminum (Al) through the process of coprecipitation,  $Zn_{1-x}Al_xO$  were formed. X-ray diffraction (XRD), Fourier transform infrared spectroscopy (FTIR), and scanning electron microscopy (SEM) analyses of all the samples supported the presence of a single crystalline phase with a hexagonal wurtzite structure. The average crystallite size in ZnO samples has decreased as a result of Al doping, while electrical conductivity and the dielectric constant have increased. According to the results of the dielectric measurement, the parameters  $k$ , or the dielectric constant or relative permittivity, and  $\tan\delta$ , or the dielectric loss, both decreased with increasing frequency.

**Keywords:** Nanoparticles; Coprecipitation; Relative permittivity; Dielectric loss; Electrical conductivity;

## Authors

### Ch. Kalyani

Research Scholar  
Department of Physics  
GITAM (Deemed to be University)  
Hyderabad, India.  
kalyani20chilamakuri@gmail.com

### Dr. IV Subba Reddy

Department of Physics  
GITAM (Deemed to be University)  
Hyderabad, India.  
isubbareddy@resiffmail.com

### Dr. P. Raju

Department of Physics  
Geethanjali College of Engineering and  
Technology  
Hyderabad, India.  
panthagansiraju@gmail.com

### Dr. P. Missak. Swarup Raju

Department of Physics  
GITAM (Deemed to be university)  
Hyderabad, India.  
Spadala4@gitam.edu

## I. INTRODUCTION

The field of nanotechnology plays a dominant role in several areas like electronics, medical technologies, etc. The changes in material properties at the nanometer scale have been explained in several ways by many researchers, that are used to develop novel, multifunctional nanomaterials suitable for device applications. Zinc oxide material attracted many researchers due to its several optical applications, such as solar cells, LEDs, photodetectors, spintronics, sensors, photocatalysis, etc. ZnO is made up of three different crystalline structures: cubic zinc blend (ZM), rock salt, and wurtzite. The wurtzite type is the most stable and stable at room temperature.

Due to the large energy band gap, transparency to visible light (400-700 nm), and some of the properties of ZnO such as electrical, optical, and acoustic, it is employed in many applications. ZnO has been prepared by various methods including the wet chemical method, hydrothermal method, chemical vapor deposition, etc. Unfortunately, pure ZnO conductivity is unstable thermally. The third group elements ( $B^{3+}$ ,  $Ga^{3+}$ ,  $Al^{3+}$ ,  $In^{3+}$ ) improve optical, electrical, thermal, and magnetic properties when they are doped in place of  $Zn^{2+}$  ions. Transparent conducting materials such as indium oxide with other dopants have been developed so far, for many optical applications.

As an alternative approach, Al-doped ZnO has been developed in the current work due to its favorable properties like non-toxic, easy availability, environmental stability, cost-effectiveness, etc. Their structural, morphological, electrical, and dielectric properties were analyzed and reported.

## II. EXPERIMENTAL

Co-precipitating method was employed to synthesize samples of ZnO containing Al dopant proportions ( $Zn_{1-x}Al_xO$ ,  $x = 0, 1\%, 3\%, 5\%, 7\%, 9\%, 10\%$ ). The primary raw materials used were  $Zn(NO_3)_2 \cdot 6H_2O$  and sodium hydroxide solution. The 0.3 M zinc nitrate solution was initially prepared by dissolving the corresponding proportions of zinc and Al dopant in 100 mL of double distilled water, by continuous stirring. Subsequently, 0.3 M of NaOH solution was dropwise added, and the stirring process continued for a period of two hours at  $75^\circ C$  before cooling to room temperature. The resultant precipitate was filtered and washed with double distilled water many times. Finally, the precipitate was again dried at  $100^\circ C$  for 24 h and then calcinated at  $700^\circ C$  for 3 h.  $Al(NO_3)_3 \cdot 9H_2O$  was added to zinc nitrate in different amounts from 1 to 10 mol%. The samples are named as ZnO, ZA01, ZA03, ZA05, ZA07, ZA09, and ZA1 for different wt% loading proportions of Al ( $x=0, 1\%, 3\%, 5\%, 7\%, 9\%, 10\%$ ), respectively. The doped samples were characterized using XRD (Philips PW-1730), FTIR (Brucker tensor 27), and SEM (LEICA, S440i, UK). The sample powders were formed into pellets measuring 10 mm in diameter and 3 mm in thickness, which were then sintered for three hours at  $1100^\circ C$ . Newton 4th Ltd. applied the silver paste to the two surfaces of sintered pellets before analyzing the dielectric characteristics with a PSM1700 meter frequency response analyzer.

## III. RESULTS AND DISCUSSIONS

X-Ray Diffraction patterns of Zinc Oxide samples substituted with aluminum in different proportions are shown in Fig. 1. The fig. shows characteristic peaks of zinc oxide

with indexing (100), (002), (101), (102), (110), (103), (112), and (201) which correspond to hexagonal wurtzite structure of ZnO. In the fig., no XRD peaks related to secondary phases of  $Al_2O_3$  or other impurities are observed which confirms the diffusion of  $Al^{3+}$  in ZnO. The figure depicts the shifting of diffraction characteristic peaks to higher angles with increasing dopant levels of  $Al^{3+}$ . The size of the crystallite was calculated from the relative intensity levels of peaks using the Scherrer equation.

$$D = k\lambda/(\beta \cos\theta)$$

Where D is the average size of the crystallite;  $\beta$  = the full width at half the diffraction peak;  $\theta$  = the Bragg angle;  $\lambda$  = the wavelength of the x-ray source; and k is the constant.

Table 1 provides an overview of the average size of crystallite for all samples, as well as the lattice parameters. It was observed that the average size decreased with the elevation of Al doping, suggesting that  $Al^{3+}$  ions were able to successfully replace  $Zn^{2+}$  ions in the structure of ZnO.

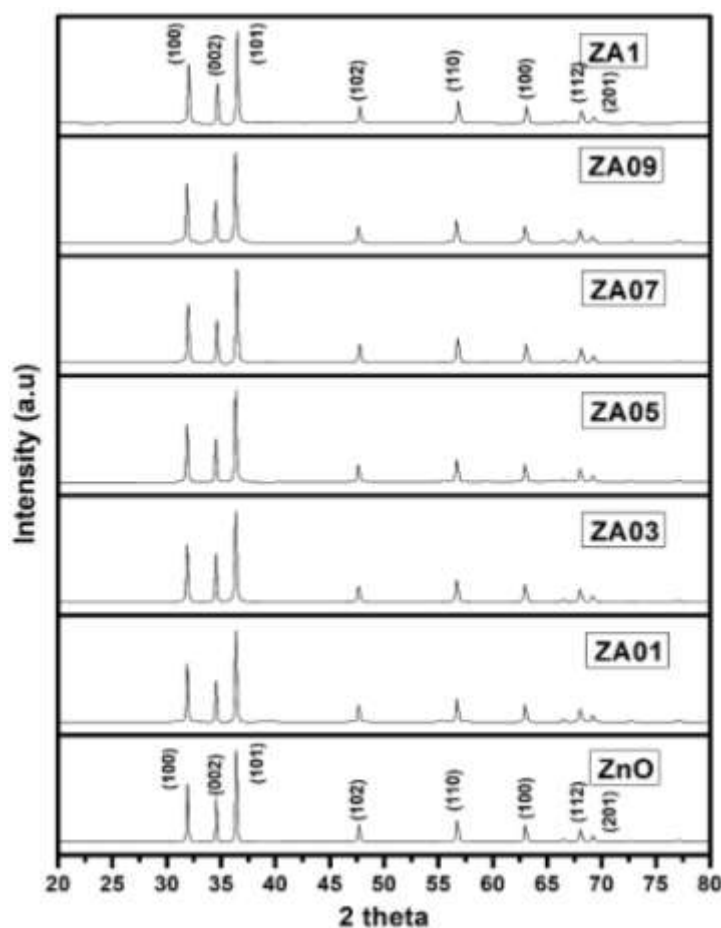


**Figure 1:** XRD Patterns Showing Zinc Oxide and ZnO Nano-Particles Substituted with Aluminum

The FTIR spectra of the ZnO samples doped with Al ranged from 4000 to 400  $cm^{-1}$ , as illustrated in Figure 2. Figure 2 indicates that the absorption band in the range 3417-3479  $cm^{-1}$  results from the stretching vibrations caused by the OH group, indicating that  $H_2O$  is

present on the sample surfaces. The band near  $500\text{ cm}^{-1}$  in figure 2 corresponds to the Zn-O stretching vibration, which aids in the production of the ZnO hexagonal wurtzite structure. Metal cations from the environment absorb  $CO_2$ , which is attributed to the bands between  $2350\text{ cm}^{-1}$  and  $1445\text{ cm}^{-1}$ . In Fig., the Al-O band is visible close to  $683\text{ cm}^{-1}$ . The change in the spectra of the doped samples depicted in fig. may be the result of Al atoms introducing crystallographic disturbance into the crystalline lattice locations. The Zn-O bond, which is present in all the prepared samples, may be identified by the band at  $445\text{ cm}^{-1}$ . As can be observed from the fig, it is discovered that the strength of the bands between  $960\text{ cm}^{-1}$  with feeble intensity and  $1122\text{ cm}^{-1}$  with high intensity increases with Al doping level. These bands match the stretching vibrations of Al-O.

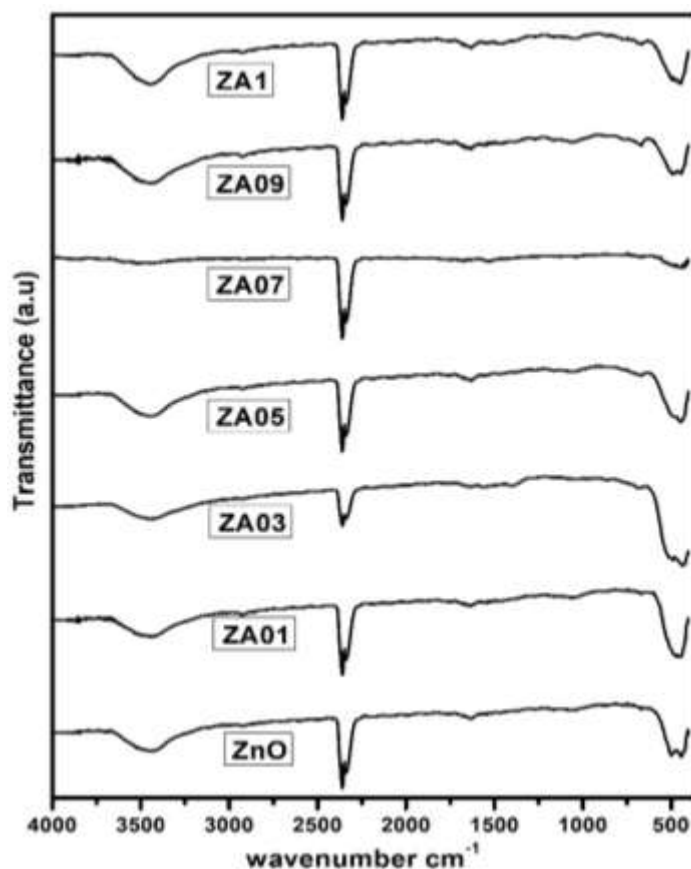


**Figure 2:** Fourier Transform Infrared Spectra of Zinc Oxide and Al-doped Zinc Oxide Nanoparticles.

The analysis of the morphological structure was performed using SEM for all samples. And the picture is shown in Fig. 3. ZnO and ZAO nanoparticles formation was seen in these micrographs. The shape of the nanoparticles is approximately spherical, and the morphology of the nanoparticles does not change after doping Al with ZnO. It has been demonstrated that agglomeration increases with the concentration of Al.

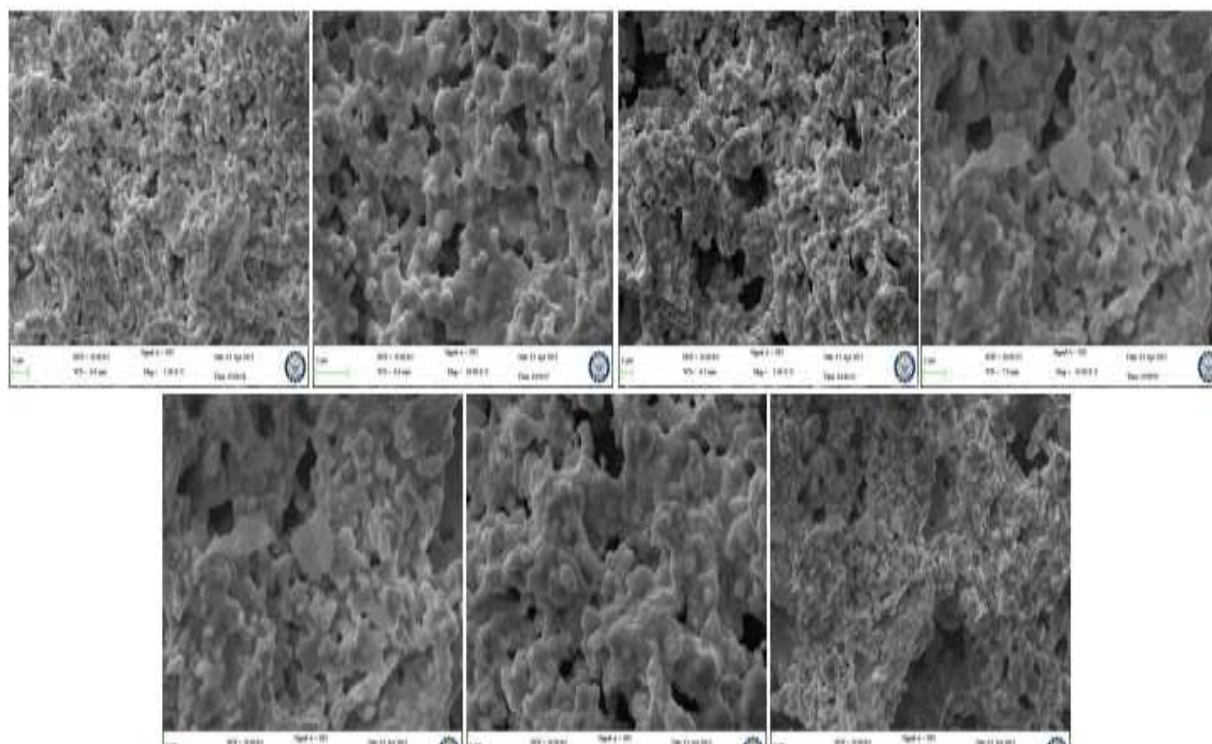


**Figure 3:** Scanning Electron Microscopy images of Zinc Oxide and Al-doped Zinc Oxide Nanoparticles.

The plots of dielectric constant  $k$  and loss versus frequency are shown in Fig. (4). The fig shows that  $k$  decreases rapidly in lower frequencies and the fall off  $k$  is slow in higher frequencies. This feature is common for all oxide nano samples.

Table 1 gives  $k$  values of all samples. The  $k$  is found to rise with Al doping amount which may be because the electro-negativity of Aluminum (1.61) is less than that of Zinc (1.78). This results in the weaker ionic bond of Zn-O-Al as compared with the Zn-O-Zn bond, which causes the increase of ionic polarization and hence dielectric constant. The average crystallite size decreases with Al concentration as noted in the table 1.

Figure 4b shows the frequency dependence of dielectric loss,  $\tan\delta$ . All samples exhibit the falling off dielectric loss with the increase of frequency at lower frequencies and at higher frequencies  $\tan\delta$  become constant. This can be attributed to ionic hopping at low and moderate frequencies leading to ionic polarization or charge carrier-induced conduction losses.

At very high frequencies, ionic vibrations are the single source that contributes to dielectric losses. Table 1 shows that dielectric losses are greatest for pure zinc oxide (ZnO) and decrease as the Al doping concentration increases. Hence, it is confirmed that doping of Al into ZnO increased the dielectric capability which is a desirable feature for high-frequency device applications.

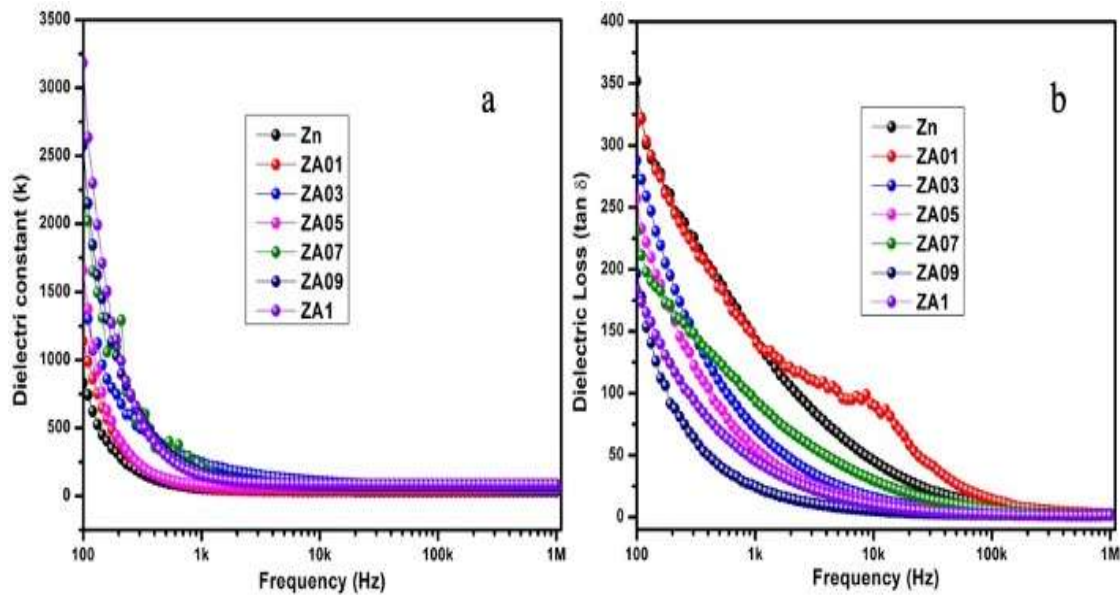


**Figure 4:** Variation of the Frequency with a) Dielectric Constant and b) Dielectric Loss ( $\tan\delta$ ) of Zinc Oxide and Al-doped Zinc Oxide Nanoparticles.

AC conductivity variation with frequency is plotted for all samples and shown in Fig. 5. As frequency increases, the number of electrons hopping cases near grain boundaries also increases which reflects an increase in AC conductivity, as seen from the fig. It can be noted from the table 1 that conductivity increases with Al doping in ZnO samples. When the Al ions are excited in the lattice of ZnO, the abundance of free charge carriers near the grain boundaries increases, resulting in high-frequency conductivity.

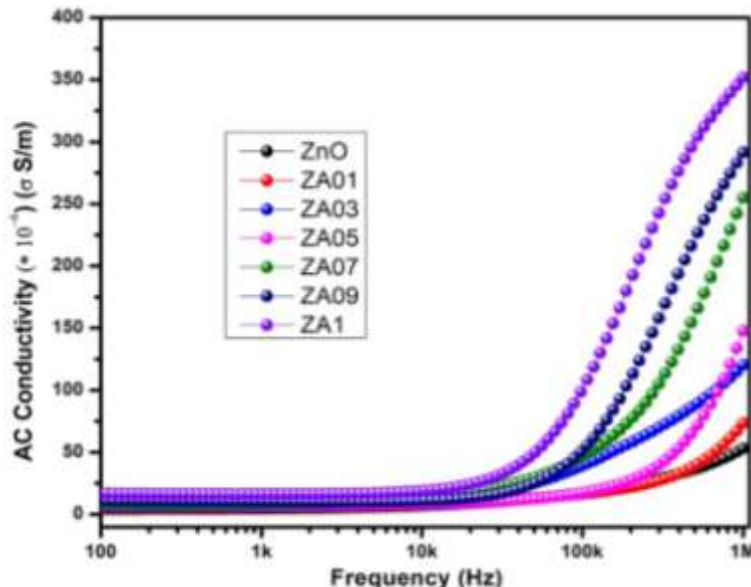


**Figure 5:** Variation of the Frequency with AC Conductivity of Zinc Oxide and Al-doped Zinc Oxide Nanoparticles.



**Table 1: Detailed Information on the Structure, Electrical Conductivity, and Dielectric Properties of Zinc Oxide and Al-doped Zinc Oxide Nanoparticles.**

Sample	Crystallite Size (nm)	Lattice parameter a (Å)	Lattice parameter c (Å)	Conductivity (S/m) at 800 kHz	Dielectric constant at 800 kHz	Dielectric Loss at 800 kHz
ZnO	79	3.235	5.603	$47.51 \times 10^{-6}$	31	2.51
ZA01	72	3.238	5.608	$61.42 \times 10^{-6}$	38	2.32
ZA03	68	3.239	5.61	$110.2 \times 10^{-6}$	45	1.94
ZA05	63	3.24	5.612	$121.01 \times 10^{-6}$	58	1.78
ZA07	59	3.229	5.594	$229.41 \times 10^{-6}$	67	1.45
ZA09	57	3.241	5.614	$274.51 \times 10^{-6}$	75	1.31
ZA1	54	3.224	5.585	$339.21 \times 10^{-6}$	84	1.14

#### IV. CONCLUSIONS

A series of samples of zinc oxide with aluminum doping, ( $Zn_{1-x}Al_xO$ ,  $x=0, 1\%, 3\%, 5\%, 7\%, 9\%, 10\%$ ), has been successfully made by co-precipitation method and confirmed by XRD, FTIR, SEM. Al doping in zinc oxide (ZnO) has been shown to improve the dielectric constant (DC) and electrical conductivity (electrical conductivity) of prepared samples with minimal dielectric losses. These features are favorable for optoelectronics and spintronics devices.

#### REFERENCES

- [1] M. Y. Ali, M. Khan, A. T. Karim, M. M. Rahman and M. Kamruzzaman, *Heliyon*, 2020, 6, e03588.
- [2] R. Sangeetha, S. Muthukumaran and M. Ashokkumar, *Spectrochim. Acta, Part A*, 2015, 144, 1–7.
- [3] K. Karthika and K. Ravichandran, *J. Mater. Sci. Technol.*, 2015, 31, 1111–1117.
- [4] K. C. Verma, in *Magnetic Materials and Magnetic Levitation*, IntechOpen, 2020.
- [5] A. B. Djurić, X. Chen, Y. H. Leung and A. M. C. Ng, *J. Mater. Chem.*, 2012, 22, 6526–6535.
- [6] R. Khan, C. I. L. de Araujo, T. Khan, S. A. Khattak, E. Ahmed, A. Khan, B. Ullah, G. Khan, K. Safeen and A. Safeen, *J. Mater. Sci.: Mater. Electron.*, 2019, 30, 3396–3404.
- [7] Nunes, P., Costa, D., Fortunato, E. and Martins, R. (2002), “Performances presented by zinc oxide thin films deposited by r.f. magnetron sputtering”, *Vacuum*, Vol. 64 No. 3-4, pp. 293-297.
- [8] Ellmer, K. (2000), “Magnetron sputtering of transparent conductive zinc oxide: relation between the sputtering parameters and the electronic properties”, *Journal of Physics D: Applied Physics*, Vol. 33 No. 4, pp. 17-32.
- [9] Lu, J.G., Ye, Z.Z., Zeng, Y.J., Zhu, L.P., Wang, L., Yuan, J., Zhao, B.H. and Liang, Q.L. (2006), “Structural, optical, and electrical properties of (Zn, Al)O films over a wide range of compositions”, *The Journal of Applied Physics*, Vol. 100 No. 073714., pp. 1-11
- [10] Kino, G.S. and Wagers, R.S. (1973), “Theory of interdigital couplers on non-piezoelectric substrates” *Journal of Applied Physics*, Vol. 44 No. 4, pp. 1480-1488.
- [11] Wang, R., King, L.L.H. and Sleight, A.W. (1996), “Highly conducting transparent thin films based on zinc oxide”, *Journal of Materials Research*, Vol. 11 No. 7, pp. 1659-1664.
- [12] Guang-hui Ning, Xiao-peng Zhao, Jia Li, Structure and optical properties of  $Mg_xZn_{1-x}O$  Nanoparticles prepared by sol-gel method, *Opt. Mater.* 27 (2004) 1-5.
- [13] H. Liu, J. Yang, Y. Zhang, L. Yang, M. Wei, X. Ding, Structure and magnetic 444 properties of Fe-doped ZnO prepared by sol-gel method, *J. Phys.: Condens. Matter* 21 (2009) 145803–145807. 446
- [14] S.S. Alias, A.B. Ismail, A.A. Mohamad, Effect of pH on ZnO nanoparticle 447 properties synthesized sol-gel centrifugation, *J. Alloy Compd.* 499 (2010) 448 231–237
- [15] M. Ahmad, E. Ahmed, Y. Zhang, Y. Khalid, X. Jianfeng, M. Ullah, Preparation of highly efficient Al-doped ZnO photocatalyst by combustion synthesis, *Curr Appl Phys* 13 (2013) 697 704.

- [16] Y. Wang, F. Luo, L. Zhang, D. Zhu, W. Zhou, Microwave dielectric properties of Al-doped ZnO powders synthesized by coprecipitation method, *Ceram Int* 39 (2013) 8723-8727.
- [17] A.A. Al-Ghamdi, O.A. Al-Hartomy, M. El-Okr, A.M. Nawar, S. El-Gazzar, F. ElTantawy, F. Yakuphanoglu, Semiconducting properties of Al-doped ZnO thin films, *Spectrochim Acta A* 131 (2014) 512-517.
- [18] A. Djelloul, M. Aida, J. Bougdira, Photoluminescence, FTIR and X-ray diffraction studies on undoped and Al-doped ZnO thin films grown on polycrystalline  $\alpha$ -alumina substrates by ultrasonic spray pyrolysis, *J Lumin*, 130 (2010) 2113-2117.
- [19] S. Maensiri, P. Laokul, V. Promarak, Synthesis and optical properties of nanocrystalline ZnO powders by a simple method using zinc acetate dihydrate and poly (vinyl pyrrolidone), *J Cryst Growth*, 289 (2006) 102-106.
- [20] A. Mishra, D. Das, Investigation on Fe-doped ZnO nanostructures prepared by a chemical route, *Mater Sci Eng B*, 171 (2010) 5-10.
- [21] N.Rajeshwari Y, A. Chandra Bose, Absorption-emission study of hydrothermally grown Al: ZnO nanostructures, *J. Alloy Compd.* 509 (2011) 8493-8500.
- [22] Imran Khan, Shakeel Kahn, Razia Nongjai, Hilal Ahmed, Wasi Khan, Structural and optical properties of gel-combustion synthesized Zr doped ZnO nanoparticles, *Opt. Mater.* 35 (2013) 1189-1193.
- [23] W.T. Kaltchev, M. Tysoe, An infrared spectroscopic investigation of thin alumina films:  
[24] measurement of acid sites and surface reactivity, *Surf. Sci.* 430 (1999) 29–36.
- [25] R. Khan, M.U. Zulfiqar, S.Fashu Rahman, Effect of annealing temperature on the dielectric and magnetic response of (Co, Zn) co-doped SnO<sub>2</sub> nanoparticles. *J. Mater. Sci.: Mater. Electron.* (2016). doi:10.1007/s10854-016-5844-z
- [26] R. Khan, Y. Zulfiqar, Zaman, Effect of annealing on structural, dielectric, transport and magnetic properties of (Zn, Co) co-doped SnO<sub>2</sub> nanoparticles. *J. Mater. Sci.: Mater. Electron.* 27, 4003–4010 (2016). doi:10.1007/s10854-015-4254-y
- R. Khan, F.M. Hu, Dielectric and magnetic properties of (Zn, Co) co-doped SnO<sub>2</sub> nanoparticles. *Chin. Phys. B* 24(12), 127803 (2015)
- [27] Suresh Sagadevan, Kaushik Pal, Zaira Zaman Chowdhury, M. Enamul Hoque., *J Sol-Gel Sci Technol* DOI 10.1007/s10971-017-4418-8
- [28] Gupta MK, Sinha N, Singh BK, Singh N, Kumar K, Kumar B (2009) Piezoelectric, dielectric, optical and electrical characterization of solution grown flower-like ZnO nanocrystal. *Mater Lett* 63:1910–1913
- [29] R. Khan, S. Zulfiqar, M.U.Rahman Fashu, Effects of Ni cooping concentrations on dielectric and magnetic properties of (Co, Ni) co-doped SnO<sub>2</sub> nanoparticles. *J. Mater. Sci.: Mater. Electron.* (2016). doi:10.1007/s10854-016-4759-z
- [30] R. Khan, S. Zulfiqar, Y.Zaman Fashu, Magnetic and dielectric properties of (Co, Zn) co-doped SnO<sub>2</sub> diluted magnetic semiconducting nanoparticles. *J. Mater. Sci.: Mater. Electron.* (2016). doi:10.1007/s10854-016-4517-2
- [31] R. Zamiri, B. Singh, M.S. Belsley, J.M.F. Ferreira, Structural and dielectric properties of Al-doped ZnO nanostructures. *Ceram. Int.* 40, 6031–6036 (2014)
- [32] C. Jayachandriah, and G. Krishnaiah, Influence of cerium dopant on magnetic and dielectric properties of ZnO nanoparticles, *J Mater Sci*, DOI 10.1007/s10853-017-0938-4.